# Influence of growth and photocatalytic properties of copper selenide (CuSe) nanoparticles using reflux condensation method

**Article** *in* Applied Surface Science · July 2013

DOI: 10.1016/j.apsusc.2013.07.022



**5 authors**, including:

Sonia S
Holy Cross College (Autonomous), Nagercoil
**8** PUBLICATIONS **34** CITATIONS
SEE PROFILE

Palaniswamy Suresh Kumar
Center of Innovation, Singapore
**64** PUBLICATIONS **1,413** CITATIONS
SEE PROFILE

Ponpandian Nagamony
Bharathiar University
**114** PUBLICATIONS **2,292** CITATIONS
SEE PROFILE

Chinnuswamy Viswanathan
Bharathiar University
**60** PUBLICATIONS **483** CITATIONS
SEE PROFILE

Applied Surface Science xxx (2013) xxx–xxx

Contents lists available at SciVerse ScienceDirect

Applied Surface Science

journal homepage: www.elsevier.com/locate/apsusc

# Influence of growth and photocatalytic properties of copper selenide (CuSe) nanoparticles using reflux condensation method

S. Sonia [a], P. Suresh Kumar [b], D. Mangalaraj [a,*], N. Ponpandian [a], C. Viswanathan [a]

[a] Department of Nanoscience and Technology, Bharathiar University, Coimbatore 641046, India
[b] Thin Film and Nanomaterials Laboratory, Department of Physics, Bharathiar University, Coimbatore 641046, India

ARTICLE INFO

*Article history:*
Received 19 April 2013
Received in revised form 24 June 2013
Accepted 6 July 2013
Available online xxx

*Keywords:*
CuSe
Reflux condensation
Nanoparticles
Photo degradation

ABSTRACT

Influence of reaction conditions on the synthesis of copper selenide (CuSe) nanoparticles and their photo degradation activity is studied. Nearly monodispersed uniform size (23–44 nm) nanoparticles are synthesized by varying the reaction conditions using reflux condensation method. The obtained nanoparticles are characterized by X-ray diffraction, field emission scanning electron microscopy, transmission electron microscopy and UV–visible absorption spectroscopy. The X-ray diffraction analysis of the sample shows the formation of nanoparticles with hexagonal CuSe structure. The result indicates that on increasing the reaction time from 4 to 12 h, the particle size decreases from 44 to 23 nm, but an increase in the reaction temperature increases the particle size. The calculated band gap $E_g$ is ranging from 2.34 to 3.05 eV which is blue shifted from the bulk CuSe (2.2 eV). The photocatalytic degradation efficiency of the CuSe nanoparticles on two organic dyes Methylene blue (MB) and Rhodamine-B (RhB) in aqueous solution under UV region is calculated as 76 and 87% respectively.



## 1. Introduction

In recent decades, hazardous environmental problems, arises from industries and modernization of the living hoods which globally affects the reusage of water and increases the demand for clean water. Among many wastewater treatment methods especially for the removal of organic contaminants, heterogeneous photocatalytic process using different nanostructures has received a considerable attention because of its low-cost and inert nature of the catalyst [1]. It is well known that the photocatalytic reaction on the surface of a semiconductor is initiated by electron and hole generation that produce hydroxyl (•OH) and superoxide (•O2-) radicals for decomposition of organic pollutant in water. So far different Nanostructured materials like ZnO, $TiO_2$, $SnO_2$, and CuO have received considerable attention due to its increase in surface areas than that of bulk materials and have been significantly investigated for both energy and environmental applications. The semiconducting photocatalysts are environmental catalysts that can efficiently degrade hazardous chemicals which have been extensively used worldwide to solve environmental issues [2–6].

As an important *p*-type semiconductor, Copper selenide (CuSe) is a unique metal chalcogenide that found in many phases and structural forms with different stoichiometries such as CuSe, $Cu_2Se$, $Cu_2Se_x$, $CuSe_2$, α-$Cu_2Se$, $Cu_3Se_2$, $Cu_5Se_4$ and $Cu_7Se_4$ as well with non-stoichiometric form such as $Cu_{2-x}Se$ and can be constructed into several crystallographic forms (monoclinic, cubic, tetragonal and hexagonal). Therefore, considerable progress on the study of CuSe has been made in recent years due to its fascinating properties and wide applications in solar cells, gas sensors, thermoelectric converters etc. Metal chalcogenide materials such as ZnSe, CuS, CuS/ZnS and CuSe modified $TiO_2$ have been directly used as photocatalysts due to their fascinating properties [7–10]. Among these, $Cu_{2-x}Se$ nanocrystals show efficient photocatalytic activity (50% with irradiation time of 2 h) towards the photodegradation of RhB aqueous solution under visible light due to its wide bandgap [11]. Among the assorted metal chalcogenides, CuSe is a *p*-type semiconductor with wide range of stoichiometric as well as non-stoichiometric compositions and also with various crystallographic forms for each of these compositions [12]. The synthesis of different nanostructures has been depicted in different methods including SILAR process, solution growth technique, brush electroplating, chemical bath deposition, chemical vapor deposition, pulsed laser deposition, thermal evaporation, solid state reaction, galvanic synthesis, solution phase synthesis and electrospinning method [13–23]. Recently, nanodendrites, nanocrystals, hollow nanostructures and nanoplates of metal chalcogenides have been synthesized by environmental friendly solvothermal method, one-pot solution, and aqueous solution method respectively [24–27]. Hydrothermal or solvothermal synthesis is a well-known low-temperature wet chemical process and it promises the direct preparation of advanced nanostructures. But the reflux condensation method provides highly crystalline materials with high purity,

* Corresponding author. Tel.: +91 422 2425458; fax: +91 422 2422387.
*E-mail address:* dmraj800@yahoo.com (D. Mangalaraj).

0169-4332/$ – see front matter © 2013 Elsevier B.V. All rights reserved.
http://dx.doi.org/10.1016/j.apsusc.2013.07.022

narrow size distribution, high surface area and low aggregation which enhance the photocatalytic activity [28]. In this paper we report the preparation of copper selenide (CuSe) nanoparticles and their photocatalytic activity on two organic dyes, viz., such as Methylene blue (MB) and Rhodamine B (RhB).

## 2. Experimental procedure

An aqueous solution of copper chloride dyhydride ($CuCl_2 \cdot 2H_2O$ (0.1 mol)) was mixed with 20 ml of ethylene glycol under vigorous stirring till it was converted to a clear solution. The pH of the resultant solution was set to 12 to make the hydroxyl ions offer stabilizing effect for the II–VI semiconductors [29]. Then 0.1 mol of selenium metal powder was dissolved in 10 ml of hydrazine hydrate and was mixed with the above solution. The moment selenide solution entered, the colourless solution suddenly changed to dark brown colour. The hydrazine hydrate acted as a reducing and complexing agent and also simultaneously a good solvent for selenium. Also, hydrazine was added to reduce any sulphite formation during the reaction. The molar ratio among Cu, Se and the stabilizer (ethylene glycol) was initially set to 1:1:2 according to the ingredients adopted in the preparations of CuSe. The resultant and final solution was refluxed in an atmospheric condition for various duration time (4, 8 and 12 h) and temperature (50 °C, 70 °C and 90 °C) respectively. The obtained precipitate was washed three times with hot double distilled water and one time with ethanol (AR grade 99.99% purity) and dried in an oven at 60 °C to remove remnants or side products. The obtained ultra fine particles were used for further investigations. The temperature and time of reactions were tuned to obtain different sized nanoparticles. The reaction mechanism is as follows:

$$CuCl_2 \xrightarrow{\text{aquous}} Cu2^{+} + 2Cl^{-}$$

$$Se \xrightarrow{\text{Reduction Ethylene Glycol/Hydrazine Hydrate}} Se^{2-}$$

$$Se^{2-} + Cu^{2+} \rightarrow CuSe$$

Phase purity, crystal structure and the crystallinity of the samples were analyzed by recording the X-ray diffraction (XRD) pattern using a Panalytical X'Pert Pro with Cu–$K_\alpha$ radiation (1.5406 Å). The UV–vis absorption and of the CuSe nanoparticles were recorded by the Perkin Elmer LS 55 fluorescence spectrometer. The surface morphology of the samples was investigated by a scanning electron microscope (SEM) (FEI Quanta-250) and the chemical composition was examined using EDAX attached with the FESEM. Also, an in-depth analysis of the morphologies of the prepared nanoparticles was done by a transmission electron microscope (TEM). The TEM image and selected area electron diffraction (SAED) pattern were recorded using a 120 KV Tecnai Sprit TEM instrument.

## 3. Results and discussion

### 3.1. Structural analysis

Fig. 1 shows the XRD pattern of the as-synthesized CuSe nanoparticles prepared at different reaction conditions such as time (4, 8 and 12 h) and temperature (50 °C, 70 °C and 90 °C) respectively. All the samples shows the sharp diffraction peaks at 26.45°, 28.15°, 31.23°, 45.92°, 50.02°, 56.51° and 70.17° can be index to (101), (102), (006), (110), (108), (116) and (208) planes of hexagonal CuSe and the intensities are very well matching with the standard JCPDS # 34-0171. No characteristic impurity peak is detected which indicates the formation of pure CuSe. All the samples show the pure hexagonal structure of CuSe with strong and sharp intensity in (102) peaks which demonstrate the better crystallization behaviour. The estimated average lattice constants are $a = 3.96$ Å and $c = 17.23$ Å, which are consistent with previously reported data and standard JCPDS value. The crystallite sizes of CuSe samples are calculated using Debye–Scherer formula as shown below in Eq. (1)

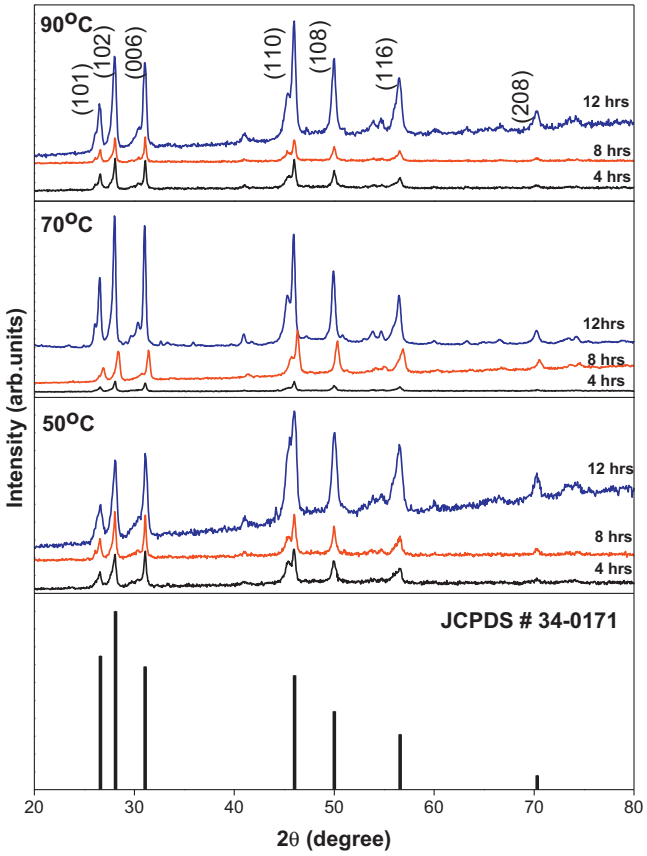


**Fig. 1.** XRD spectra of CuSe nanoparticles refluxed at different reaction temperature and time.

$$D = \frac{0.89\lambda}{\beta \cos\theta} \quad (1)$$

where $D$ is the crystallite size, $\lambda$ is the wavelength (1.5406 Å for Cu–Kα), $\beta$ is the full-width at half-maximum (FWHM) of main intensity peak after subtraction of the equipment broadening and $\theta$ is the diffraction angle. It is interesting to note that the average crystallite size decreases by increasing the reaction time from ~44.73 (for 4 h) to ~23.73 nm (for 12 h) and no appreciable change in crystallite size is noticed in the reaction time of 12 h and at the reaction temperatures of 50, 70 and 90 °C. The reaction time plays an important role in determining the surface structure of the nanoparticles. When the reaction time increases, faster growth rate of the nanoparticles can reduce the surface defects of the nanoparticles, but lower reaction time would reduce the reaction speed which in turn may adversely influence the quality of the nanoparticles [30]. Generally, the monomer reactivity was a function of reaction temperature. Therefore, it was understood that the reaction temperature could affect the reactivity of Se and, thereby, the nucleation process of NPs. When the temperature was low, the reactivity of Se was not high enough to support the reaction with Cu. When the temperature is high the diffraction peaks show high crystallinity of CuSe nanoparticles compared to the growth of nanoparticles at low temperatures due to the high reactivity of Se with Cu [31].

Please cite this article in press as: S. Sonia, et al., Influence of growth and photocatalytic properties of copper selenide (CuSe) nanoparticles using reflux condensation method, Appl. Surf. Sci. (2013), http://dx.doi.org/10.1016/j.apsusc.2013.07.022

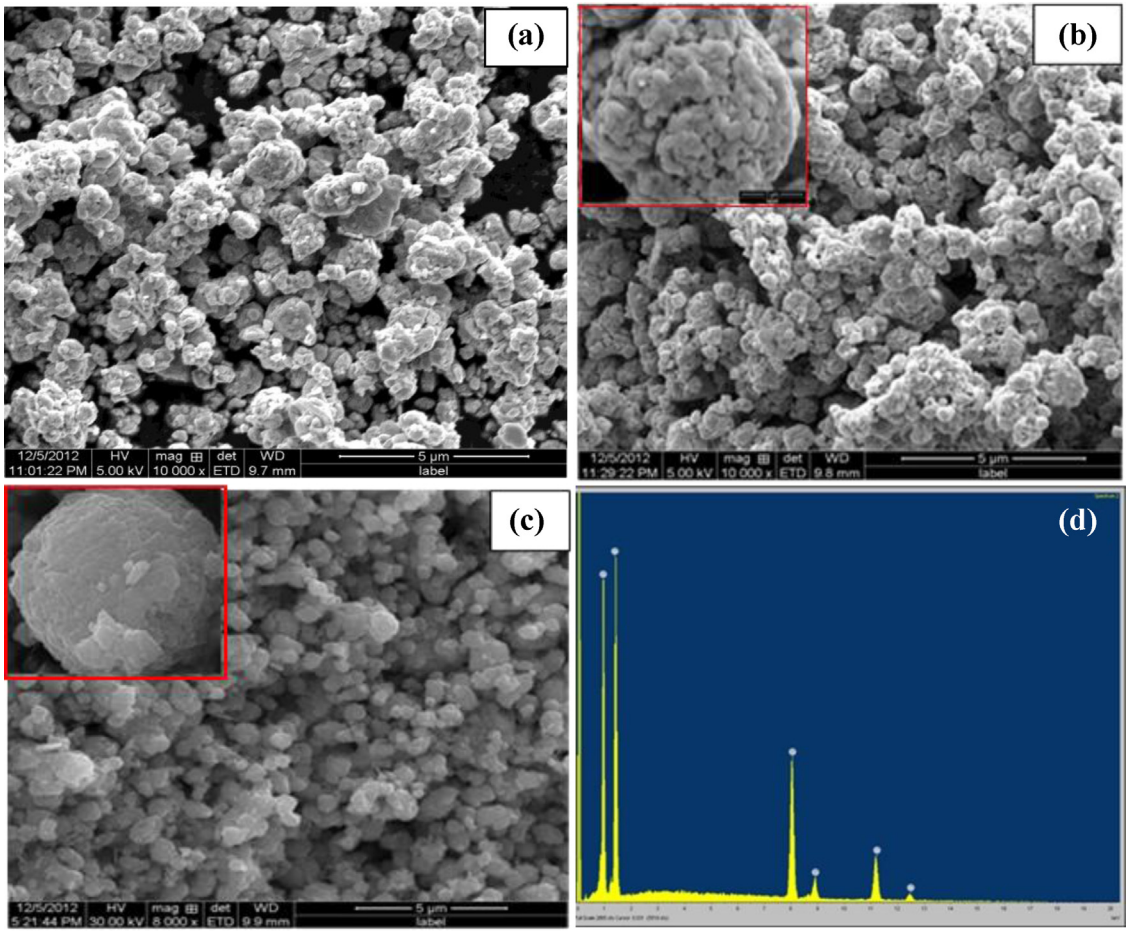


**Fig. 2.** SEM image of CuSe refluxed at different reaction temperature (a) 50 °C (b) 70 °C (c) 90 °C and time of 12 h (d) EDX analysis of CuSe nanoparticle synthesized at rection temperature of 90°c for 12 h.

### 3.2. Surface and compositional analysis

The surface morphology of the prepared CuSe nanoparticles were analyzed by scanning electron microscopy (SEM). The sample synthesized at lower reaction temperature (50 °C) shows the formation of irregular structures upto 2 μm (Fig. 2(a)) whereas the sample refluxed at higher temperature of 70 °C typically shows the porous CuSe nanoparticles as shown in inset Fig. 2(b) with size ranging from 1 to 1.5 μm which aggregate into bunch of clusters (Fig. 2(b)). The morphology of these samples reveals that the agglomeration of nanocrystals leads to the formation of individual particles or grains, which are expected to contribute more grain boundary effects. Further increase in reaction temperature (90 °C) evidently shows the spherical CuSe nanoparticle with size ranges from 200 nm to 1 μm (Fig. 2(c)). These spherical particles are highly crystalline in nature. The EDAX spectrum shows the presence of Cu and Se elements alone in the sample, confirming the absence of any other impurity. The atomic percentage of Cu and Se elements sample is 53.43 and 46.57, respectively are shown in Fig. 2(d). The stoichiometric ratio calculated from the EDAX is 1:1 shows the presence of pure CuSe.

The size and shape of the CuSe nanoparticles are depicted in the TEM image (Fig. 3(a)). The typical TEM image shows that the shape of the copper selenide nanoparticles is spherical, with the average particle size of 20–40 nm which is coincidence with the average grain size calculated from the XRD pattern. The TEM image of the sample shows nearly spherical morphology and good monodispersity. The selected area electron diffraction (SAED) pattern of the sample (Fig. 3(b)) shows the discontinuous diffraction rings, suggesting that the crystalline domains of the nanocrystalline powders have certain preferred orientations instead of the random orientations. This diffraction pattern exhibits a typical lattice spacing of about 3.160, 2.625, 1.791 and 1.603 Å, corresponding to the planes (102), (006), (108) and (116) respectively, which are confirmed with the XRD results.

### 3.3. Optical analysis

The optical absorption peaks of the CuSe nanoparticles prepared with different reaction parameters are shown in Fig. 4(a–c). In the present case, the absorption is maximum at 350 nm for the material prepared with a reaction time of 12 h and a reaction temperature of 50 °C. This peak is related to the plasmon band of the nano-sized copper selenide particles (Fig. 4(a)). Fig. 4 (b) indicates that as the temperature of copper selenide increases to 70 °C, the absorption band becomes stronger and sharper. Further it moves to a shorter wavelength of 345 nm. This indicates that the size of the nanoparticles is decreasing when the temperature is increased. As the temperature of the copper selenide is increased to 90 °C, the absorption band is shifted towards shorter wavelength of 344 nm (Fig. 4(c)) and also the peak become very stronger and sharper compared to the peak obtained in the reaction temperatures 50 °C and 70 °C. In every case, the absorption peak shifts towards lower wavelength as the temperature of the copper selenide is increased. The peak also gets stronger. This is probably because of reduction in the particle size and hence increases in the surface to volume ratio.

Please cite this article in press as: S. Sonia, et al., Influence of growth and photocatalytic properties of copper selenide (CuSe) nanoparticles using reflux condensation method, Appl. Surf. Sci. (2013), http://dx.doi.org/10.1016/j.apsusc.2013.07.022

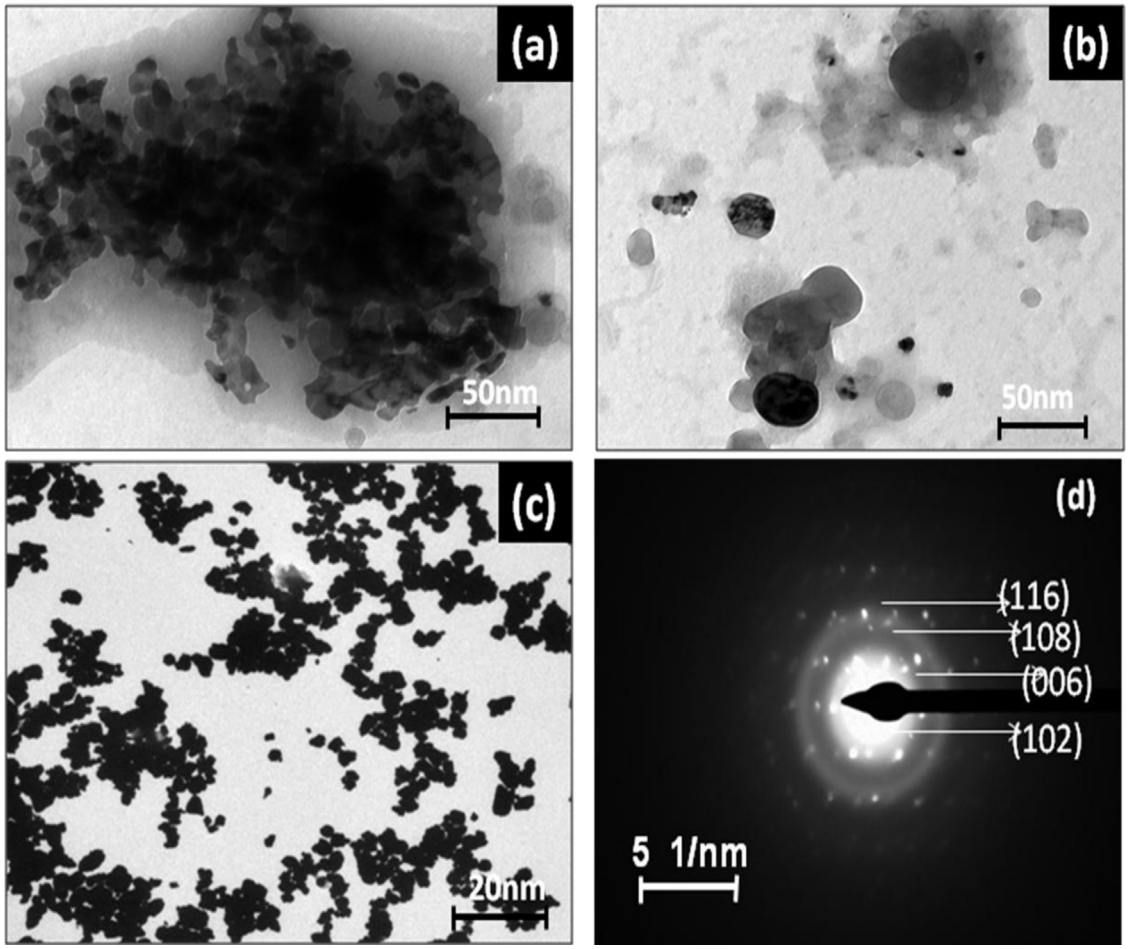


**Fig. 3.** TEM image of CuSe refluxed at different reaction temperature (a) 50 °C (b) 70 °C (c) 90 °C and time of 12 h (d) SAED pattern of CuSe nanoparticles refluxed at reaction temperature of 90 °C and time of 12 h.

Also it may be due to the confinement of electron and hole in a very small volume [32]. In Fig. 4(a–c) no sharp absorption edge is observed at large wavelengths. The set of sharp absorption peaks at shorter wavelengths is due to exciton absorption and confinement of electron and hole. The sharp absorption edge implies that the particles are spherical in shape [33–35]. The stronger exciton effect is an important character of the quantum confinement effect in nano-semiconductors, since the carriers are confined in a very small region that makes the electron and holes move only in a potential well. At the same time, it can enhance the coupling interaction, due to which the excitons are bounded more strongly. Hence the probability of binding is increased, which lead to apparent exciton absorption peak and hence the blue shift. Usually, the optical absorption at the absorption edge corresponds to the transmission from valence band to conduction band, while the absorption in the visible region corresponds to some localized energy states in the band gap. The optical band gap was calculated by plotting $\alpha h\nu$ (vs) $h\nu$ plot. For forbidden electronic transition in materials, the absorption coefficient $\alpha$ is given by

$$\alpha h\nu = k(h\nu - E_g)^p \quad (2)$$

where $p = 1/2$ for direct forbidden gap and $p = 3$ for indirect forbidden gap [18,22,36]. $(\alpha h\nu)^{1/2}$ versus $h\nu$ plots for CuSe prepared at different temperatures and reaction timings are shown in Fig. 5(a–c). Good linear relationship between $(\alpha h\nu)^{1/2}$ and $h\nu$ indicates that the nature of transition in CuSe nanoparticles is direct transition. The band gap $E_g$ calculated by extrapolating the linear part of the curve to zero absorption is ranging from 2.34 to 3.05 eV which is blue shifted from the bulk CuSe (2.2 eV) [18,20] and this blue shift is due to quantum confinement effect. From Fig. 5(a–c) it is clear that as the particle size decreases the band gap gets increased. Nanosize effect and the structural defects might lead to the blue shift of the copper selenide nanoparticles [32].

### 3.4. Photocatalytic activity

Fig. 6(a–b) shows the photo-degradation activity of the prepared CuSe nanoparticles was examined against two organic dyes, viz., Methylene blue (MB) and Rhodamine-B (RhB) for the optimized sample prepared at reaction temperature (90 °C) and time (12 h). Photocatalysis refers to the oxidation and reduction reactions on semiconductor surfaces, mediated by the valance band holes and conduction band electrons, which are generated by the absorption of ultraviolet or visible light radiation. In a typical experiment, 3 mg of CuSe was dissolved in 1 mole aqueous solutions of RhB and MB. In order to make homogeneous dispersion, the solutions are sonicated for 20 min. The resultant solution was kept in a dark condition to obtain equilibrium between the catalyst and organic (RhB and MB) molecules. Then the solution was illuminated by a UV light source ($\lambda_{max} = 365$ nm) to induce photochemical reaction. Strong absorption peaks at 554 and 665 nm are observed for RhB and MB respectively.

As seen in the figures, a substantial decrease in the absorbance of dyes (RhB and MB) was observed after conducting the reaction under UV light irradiation. The solution turned colourless within

Please cite this article in press as: S. Sonia, et al., Influence of growth and photocatalytic properties of copper selenide (CuSe) nanoparticles using reflux condensation method, Appl. Surf. Sci. (2013), http://dx.doi.org/10.1016/j.apsusc.2013.07.022

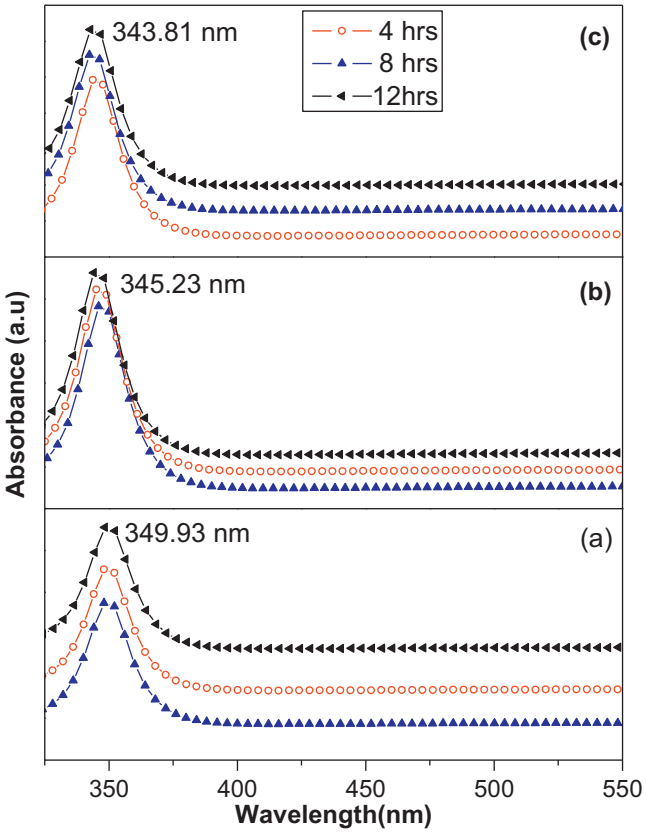


**Fig. 4.** Optical absorption spectra of CuSe nanoparticles refluxed at different reaction temperatures (a) 50 °C (b) 70 °C and (c) 90 °C.

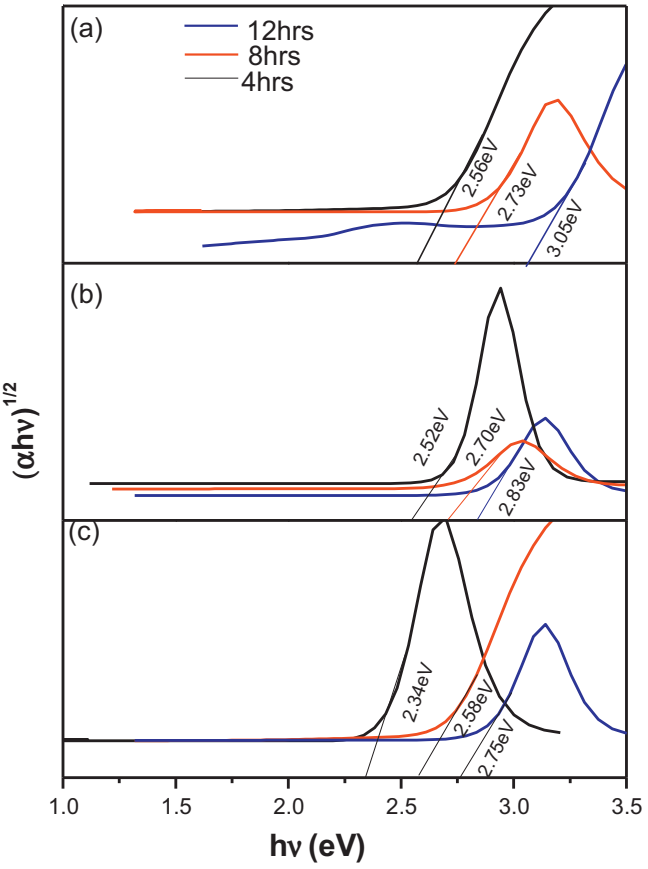


**Fig. 5.** Plot of $(\alpha h\nu)^{1/2}$ vs $h\nu$ of CuSe nanoparticles refluxed at different reaction temperatures (a) 50 °C (b) 70 °C and (c) 90 °C.

90 min of irradiation. The efficiency of degradation ($\eta$ %) was calculated using

$$\eta(\%) = (1 - A/A_0) \times 100, \quad (3)$$

Where, $A_0$ is the absorption maximum at $t = 0$, $A$ be the absorption maximum after degradation for a particular illumination time. Fig. 7(a) shows the changes of RhB and MB concentration ratio ($A/A_0$) as a function of illumination time. Fig. 7(b) shows that the degradation percentage increases as the UV irradiation time increases. The degradation efficiency for the CuSe nanoparticles with the RhB and MB are calculated as 87 and 76% respectively. The highest degradation was achieved for RhB than MB. The photocatalytic degradation of the organic dyes by the CuSe nanoparticles under UV light obeyed pseudo-first order kinetics with respect to the absorption intensity of dyes:

$$-dA/dt = k_{app}A \quad (4)$$

Integration of the equation (with $A = A_{abs}$ at $t = 0$, with $A_{abs}$ being the initial concentration in the bulk solution after dark adsorption and $t$ the reaction time) lead to

$$-\ln(A/A_0) = k_{app}\, t \quad (5)$$

where $A$ and $A_0$ are the absorption intensities at time $t = t$ and $t = 0$ respectively, $k_{app}$ and $t$ are the apparent reaction rate constant and time respectively. Accordingly, a plot of $-\ln(A/A_0)$ versus $t$ will yield a slope of $k_{app}$ and results are shown in Fig. 8. The linearity of the plot suggested that the photodegradation reaction approximately followed pseudo-first order kinetics with $k_{app}$ of 0.0155 $min^{-1}$ and 0.0174 $min^{-1}$ for degradation of MB and RhB respectively. The result suggests that the CuSe nanoparticles are effective catalysts for RhB and MB degradation.

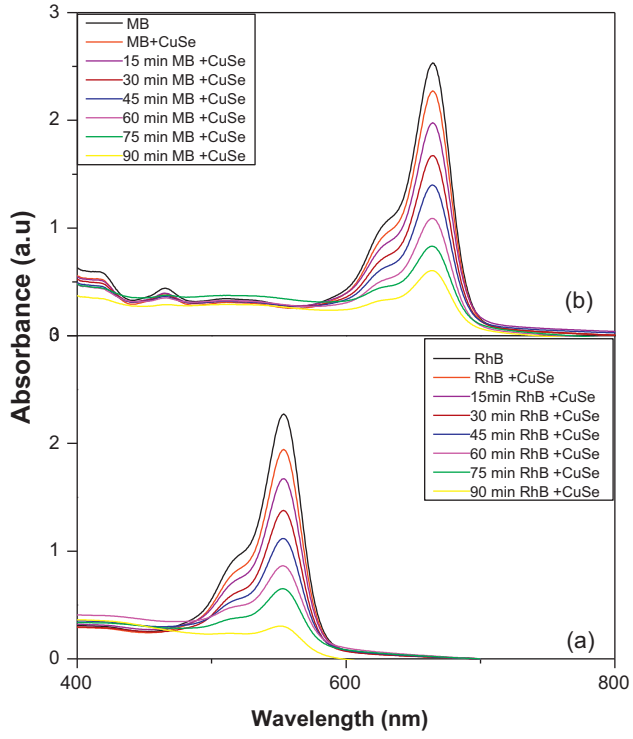


**Fig. 6.** Photo-degradation of CuSe nanoparticles of two organic dyes (a) RhB and (b) MB.

Please cite this article in press as: S. Sonia, et al., Influence of growth and photocatalytic properties of copper selenide (CuSe) nanoparticles using reflux condensation method, Appl. Surf. Sci. (2013), http://dx.doi.org/10.1016/j.apsusc.2013.07.022

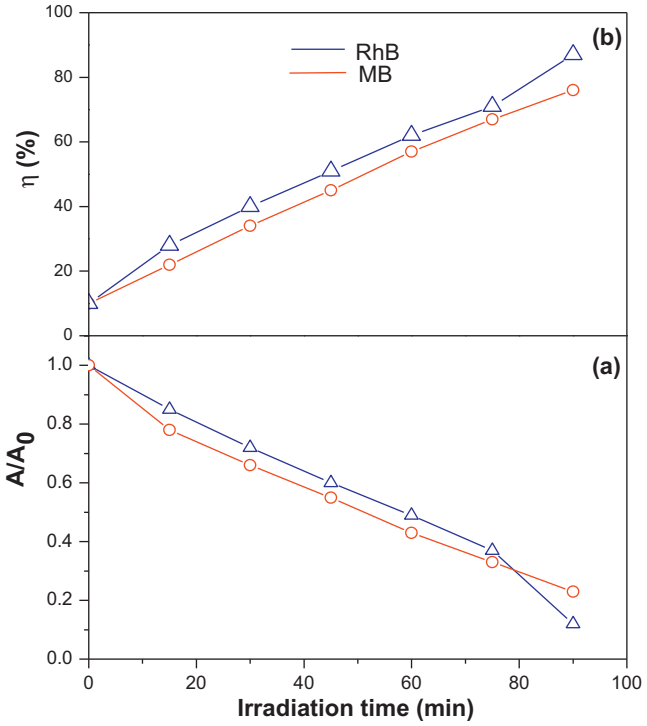


**Fig. 7.** (a) Changes of RhB and MB concentration ratio C/C0 as a function of illumination time (b) Degradation efficiency of two organic dyes by the CuSe nanoparticles under UV irradiation.

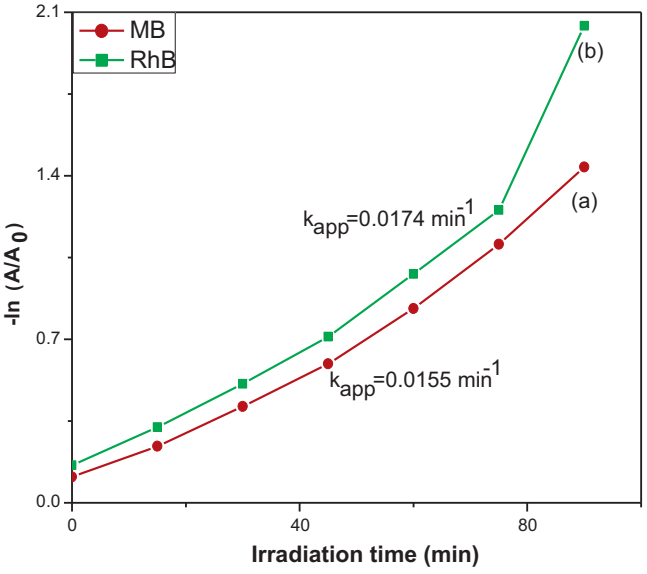


**Fig. 8.** First order kinetics plot for the photodegradation of (a) MB and (b) RhB by CuSe nanoparticles under UV light irradiation.

## 4. Conclusion

In summary, highly crystalline CuSe nanoparticles have been prepared using cost effective reflux condensation method by varying the reaction time and temperature. The XRD analysis confirms the phase purities with (102) peak orientation of CuSe with crystallite size varying from 22 nm to 9 nm with change in reaction condition. The optical studies confirm the strong blue shift is due to the quantum confinement effect. The prepared CuSe had excellent photocatalytic properties and the photocatalytic degradation efficiency of the nanoparticles on two organic dyes Methylene blue (MB) and Rhodamine-B (RhB) in aqueous solution under UV region is found to be around 76 and 87% respectively.

## References

[1] N. Murase, R. Jagannathan, Y. Kanematsu, M. Watanabe, A. Kurita, K. Hirata, T. Yazawa, T. Kushida, The Journal of Physical Chemistry B 103 (1999) 754.
[2] K. Honda, A. Fujishima, Nature 238 (1972) 37–38.
[3] T. Kawai, T. Sakata, Nature 286 (1980) 474–476.
[4] T. Mishra, J. Hait, Noor Aman, R.K. Jana, S. Chakravarty, Journal of Colloid and Interface Science 316 (2007) 80–84.
[5] D. Wang, Z. Zou, J. Ye, Chemical Physics Letters 384 (2004) 139–143.
[6] A.L. Linsebigler, G. Lu, J.T. Yates, Chemical Review 95 (1995) 735–758.
[7] S. Cho, J.W. Jang, J. Kim, J.S. Lee, W. Choi, K.H. Lee, Langmuir 27 (2011) 10243–10250.
[8] L. Zhang, H. Yang, J. Yu, F. Shao, L. Li, F. Zhang, H. Zhao, The Journal of Physical Chemistry B 113 (2009) 5434–5443.
[9] J. Yu, J. Zhang, S. Liu, The Journal of Physical Chemistry B 114 (2010) 13642–13649.
[10] Y. Li, S. Luo, L. Yang, C. Liu, Y. Chen, D.S. Meng, Electrochimica Acta 83 (2012) 394–401.
[11] T.D.T. Ung, Q.L. Nguyen, Advances in Natural Sciences: Nanoscience and Nanotechnology 2 (2011) 045003.
[12] G.B. Sakra, I.S. Yahia, M. Fadel, S.S. Fouad, N. Romcevi, Journal of Alloys and Compounds 507 (2010) 557–562.
[13] P.S. Kumar, J. Sundaramurthy, D. Mangalaraj, D. Nataraj, D. Rajarathnam, M.P. Srinivasan, Journal of Colloid and Interface Science 363 (2011) 51–58.
[14] P.S. Kumar, A. Dhayal Raj, D. Mangalaraj, D. Nataraj, Applied Surface Science 255 (2008) 2382–2387.
[15] K.R. Murali, R. John Xavier, Chalcogenide Letters 6 (2009) 683–687.
[16] R.H. Bari, V. Ganesan, S. Potadar, L.A. Patil, Bulletin of Material Science 32 (2009) 37–42.
[17] A.B.M.O. AL-Mamun, A.H. Islam, Bhuiyan, Journal of Materials Science: Materials in Electronics 16 (2005) 263–268.
[18] Y. Hu, M. Afzaal, M.A. Malik, P. O'Brien, Journal of Crystal Growth 297 (2006) 61–65.
[19] M.Z. Xue, Y.N. Zhou, B. Zhang, L. Yu, H. Zhang, Z.W. Fu, Journal of The Electrochemical Society 153 (2006) A2262–A2268.
[20] Y.J. Yang, S. Hu, Journal of Solid State Electrochemistry 13 (2009) 477–483.
[21] R. Seoudi, A.A. Shabaka, M.M. Elokr, A. Sobhi, Materials Letters 61 (2007) 3451–3455.
[22] P. Kumar, K. Singh, O.N. Srivastava, Journal of Crystal Growth 312 (2010) 2804–2813.
[23] P.S. Kumar, S.A. Syed Nizar, J. Sundaramurthy, P. Ragupathy, V. Thavasi, S.G. Mhaisalkar, S. Ramakrishna, Journal of Materials Chemistry 21 (2011) 9784–9790.
[24] D. Li, Z. Zheng, Y. Lei, S. Ge, Y. Zhang, Y. Zhang, K.W. Wong, F. Yanga, W.M. Lauc, CrystEngComm 12 (2010) 1856–1861.
[25] G. Xiao, J. Ning, Z. Liu, Y. Sui, Y. Wang, Q. Dong, W. Tian, B. Liu, G. Zou, B. Zou, CrystEngComm 14 (2012) 2139.
[26] M.S. Bakshi, P. Thakur, P. Khullar, G. Kaur, T.S. Banipal, Crystal Growth and Design 10 (2010) 4.
[27] G. Xiao, Y. Zeng, Y. Jiang, J. Ning, W. Zheng, B. Liu, X. Chen, G. Zou, B. Zou, Small 9 (2013) 793–799.
[28] D. Chen, Recent Patents on Nanotechnology 2 (2008) 183–189.
[29] D. Zhao, Z. He, W.H. Chan, M.M.F. Choi, The Journal of Physical Chemistry 113 (2009) 1293–1300.
[30] P.K. Basu, Theory of Optical Processes in Semiconductors Bulk and Microstructure, Clarendon Press, Oxford, 1997.
[31] W.W. Yu, Y.A. Wang, X. Peng, Chemistry of Materials 15 (2003) 4300–4308.
[32] M.N. Kalasad, M.K. Rabinal, B.G. Mulimani, Langmuir 25 (2009) 12729–12735.
[33] A. Moores, F. Goettmann, New Journal of Chemistry 30 (2006) 1121.
[34] S. Link, M.A. El-Sayed, The Journal of Physical Chemistry 3 (2000) 409.
[35] C.S. Prajapati, P.P. sahay, Journal of Applied Surface Science 258 (2011) 2823–2826.
[36] B. Pejova, I. Grozdanov, Journal of Solid State Chemistry 158 (2001) 49–54.

Please cite this article in press as: S. Sonia, et al., Influence of growth and photocatalytic properties of copper selenide (CuSe) nanoparticles using reflux condensation method, Appl. Surf. Sci. (2013), http://dx.doi.org/10.1016/j.apsusc.2013.07.022